Observational Study

Medicine®

OPEN

Predicting chemoradiotherapy response of nasopharyngeal carcinoma using texture features based on intravoxel incoherent motion diffusion-weighted imaging

Yuhui Qin, BA[a], Xiaoping Yu, MD[a,*], Jing Hou, MM[a], Ying Hu, MM[b], Feiping Li, MM[a], Lu Wen, MM[a], Qiang Lu, BA[a], Yi Fu, MM[c], Siye Liu, BA[a]

Abstract

The aim of the study was to investigative the utility of gray-level co-occurrence matrix (GLCM) texture analysis based on intravoxel incoherent motion diffusion-weighted imaging (IVIM-DWI) for predicting the early response to chemoradiotherapy for nasopharyngeal carcinoma (NPC).

Baseline IVIM-DWI was performed on 81 patients with NPC receiving chemoradiotherapy in a prospective nested case–control study. The patients were categorized into the residue (n = 11) and nonresidue (n = 70) groups, according to whether there was local residual lesion or not at the end of chemoradiotherapy. The pretreatment tumor volume and the values of IVIM-DWI parameters (apparent diffusion coefficient [ADC], D, D^*, and f) and GLCM features based on IVIM-DWI were compared between the 2 groups. Receiver operating characteristic (ROC) curves in univariate and multivariate logistic regression analysis were generated to determine significant indicator of treatment response.

The nonresidue group had lower tumor volume, ADC, D, $Correlat_{ADC}$, $Correlat_D$, $InvDfMom_{ADC}$, $InvDfMom_D$ and $InvDfMom_D^*$ values, together with higher $Contrast_D$, $Contrast_f$, $SumAverg_{ADC}$, $SumAverg_D$, and $SumAverg_D^*$ values, than the residue group (all $P < .05$). Based on ROC curve in univariate analysis, the area under the curve (AUC) values for individual GLCM features in the prediction of the treatment response ranged from 0.635 to 0.879, with sensitivities from 54.55% to 100.00% and specificities from 52.86% to 85.71%. Multivariate logistic regression analysis demonstrated D ($P = .026$), $InvDfMom_{ADC}$ ($P = .033$) and $SumAverg_D$ ($P = .015$) as the independent predictors for identifying NPC without residue, with an AUC value of 0.977, a sensitivity of 90.91% and a specificity of 95.71%.

Pretreatment GLCM features based on IVIM-DWI, especially on the diffusion-related maps, may have the potential to predict the early response to chemoradiotherapy for NPC.

Abbreviations: ADC = apparent diffusion coefficient, AngScMom = angular second moment, AUC = area under the curve, D^* = pseudo-diffusion coefficient, D = pure diffusion coefficient, DifEntrp = difference entropy, Difvarnc = difference variance, DWI = diffusion-weighted imaging, f = perfusion fraction, GLCM = gray-level co-occurrence matrix, InvDfMom = inverse difference moment, IVIM-DWI = intravoxel incoherent motion diffusion-weighted imaging, MRI = magnetic resonance imaging, NPC = nasopharyngeal carcinoma, ROC = receiver operating characteristic, ROI = region of interest, SumAverg = sum average, SumEntrp = sum entropy, SumOfSqs = sum of squares, SumVarnc = sum variance, VOI = volume of interest.

Keywords: chemoradiotherapy, diffusion magnetic resonance imaging, nasopharyngeal neoplasms, radiographic image interpretation, treatment outcome

Editor: Cheng-Chia Yu.

This study was supported by the Provincial Key Clinical Specialty (Medical Imaging) Development Program from Health and Family Planning Commission of Hunan Province, China (contract grant number: 2015/43), and by the Guidance Program for Clinical Technique Innovation from Provincial Science and Technology Department, Hunan, China (project number: 2017SK50601).

The authors have no conflicts of interest to disclose.

[a] Department of Diagnostic Radiology, [b] Department of Radiotherapy, [c] Department of Medical Service, The Affiliated Cancer Hospital of Xiangya School of Medicine, Central South University and Hunan Cancer Hospital, Changsha, Hunan, China.

[*] Correspondence: Xiaoping Yu, Department of Diagnostic Radiology, The Affiliated Cancer Hospital of Xiangya School of Medicine, Central South University and Hunan Cancer Hospital, 283 Tongzipo Road, Yuelu District, Changsha 410013, Hunan, China (e-mail: yuxiaoping@hnszlyy.com).

Medicine (2018) 97:30(e11676)

Received: 14 February 2018 / Accepted: 5 July 2018

http://dx.doi.org/10.1097/MD.0000000000011676

1. Introduction

As a tumor with a noticeable geographic and racial distribution worldwide, nasopharyngeal carcinoma (NPC) is a common malignancy of head and neck in South China, such as Guangxi and Guangdong provinces.[1,2] In most areas worldwide, annual incidence of NPC is <1 per 100,000 for both sexes, for example, 0.5 and 0.2 per 100,000 person-years for male and female in the United States, respectively.[1] However, the newly reported incidence of NPC in Guangxi and Guangdong is about 11 per 100,000.[2] Chemoradiotherapy is currently regarded as the preferred treatment for locally advanced NPC as it can decrease the local recurrence rate and subsequently achieve significant survival benefit.[3,4] However, local failure (ie, residue or recurrence) remain one of the predominant patterns of treatment failure in patients with NPC.[5] Predicting therapeutic response to chemoradiotherapy as early as possible has remarkable clinical benefit for patients with NPC, which could optimize treatment regimen, avoid unnecessary suffering from chemoradiotherapy toxicity, and reduce medical cost.

Nowadays, magnetic resonance imaging (MRI) is playing an increasingly important role in lesion detection, clinical staging, and therapeutic effect evaluation and prediction for NPC.[6–9] Convention morphology-based MRI offers little benefit in the early prediction of therapeutic effect in NPC. Recently, functional MRI approaches including dynamic contrast-enhanced MRI and diffusion-weighted imaging (DWI) have been utilized to predict the treatment response for NPC.[8,10–12] Nevertheless, previous studies have demonstrated variable efficacy of dynamic contrast-enhanced MRI and DWI in early predicting the response of NPC to chemoradiotherapy.[8,10–15] These controversial results might result from that these MRI approaches were based on the analysis of mean value of MRI parameter, which cannot accurately reflect histologic heterogeneity. Heterogeneity is a common phenomenon in malignancies and it is strongly linked with curative effect of NPC.[16,17] Texture features derived from MRI have the ability to quantitate tumor heterogeneity.[16,18–20] Some published studies have demonstrated the advantage of texture features over the analysis of morphology-based MRI and mean value of MRI parameter in discriminating clinical stage or treatment response for a variety of tumors.[21–24]

Up to now, most of the available MRI literatures on texture analysis were based on morphologic image, although several on dynamic contrast-enhanced MRI or the apparent diffusion coefficient (ADC) map derived from DWI.[16,20,21] Morphologic image cannot provide functional information of tissue microstructure, which may limit its potential to early predict treatment response of tumors. In regard to the ADC value, it is obtained from a mono-exponential diffusion model and only reflects hybrid diffusion information resulting from both Brownian movement and microcirculation perfusion. Intravoxel incoherent motion DWI (IVIM-DWI), with the ability to separate pure diffusion movement and perfusion, was found to be more powerful than the ADC value in predicting the curative effect of NPC.[11,12]

The utility of texture features derived from IVIM-DWI in predicting the response to chemoradiotherapy of NPC is still unknown until now. Gray-level co-occurrence matrix (GLCM) is a widely used texture analysis algorithm which generates texture features to quantify the spatial gray-level variation within local neighborhoods around each pixel in an image.[21,25–27] GLCM features have shown promise in predicting the treatment response in many kinds of tumors.[20,26,28,29] Therefore, we hypothesize that GLCM analysis based on IVIM-DWI has a capacity to predict the early response to chemoradiotherapy for NPC, which is still unclear until now according to the best of our knowledge. The aim of this study was to investigate this capacity of GLCM approach.

2. Materials and methods

2.1. Patient selection and treatment procedure

This prospective single-center study was approved by the Medical Ethics Committee in our institution, and all patients with NPC signed written informed consent. Inclusion criteria of this study were as follows: newly diagnosed and pathologically confirmed of nonkeratinizing NPC, above 18 years old, patients were scheduled for chemoradiotherapy, and Karnofsky score ≥80. Patients were excluded if they had prior antitumor treatment for NPC, did not sign the informed consent form, or had contraindications for MRI. Ninety patients with NPC were initially enrolled from September 2016 to April 2017 (Fig. 1). All patients' clinical stages were determined with reference to the 7th edition of the International Union Against Cancer/American Joint Committee on Cancer (UICC/AJCC) staging system.[30]

All patients received a 2-cycle induction chemotherapy (21 days per cycle) that consisted of 135 to 175 mg/m^2 paclitaxel on day 1 accompanied by 80 mg/m^2 nedaplatin on days 1, 2, and 3. After induction chemotherapy, all patients received radiotherapy with a total dose of 70 to 76 Gy and 30 to 33 times to completion. After radiotherapy, 2 head and neck radiologists (LF and HJ with 15 and 6 years of experience in neck radiology, respectively) who were blinded to the texture analysis data read the MRIs individually and classified the patients with NPC into the residue and nonresidue groups, with a double-blind control, according to whether regional residue was identified on MRI and pharyngorhinoscopy which were performed at the end of chemoradiotherapy. If they have different views of residual tumor, the third neck radiologist (YX with more than 20 years of experience in neck radiology) would analysis these data and eventually determined whether there was residue or not.

2.2. MRI protocols

Before chemoradiotherapy, all patients received conventional MRI and IVIM-DWI examinations on a 1.5 Tesla MRI scanner

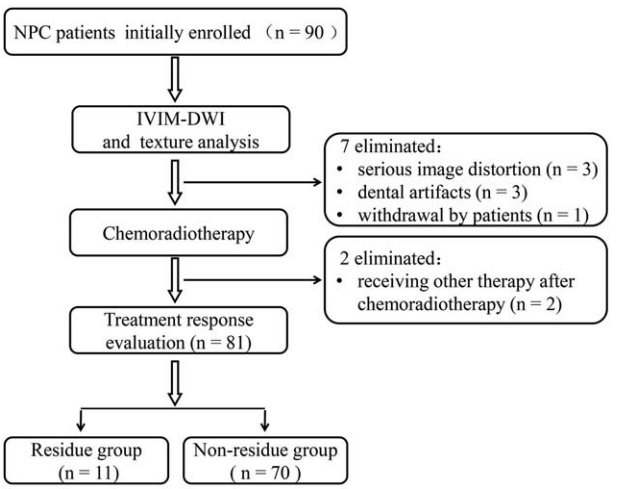

Figure 1. Study flow diagram in this study.

(Optima MR360; GE Healthcare, Milwaukee, WI). The conventional MRI protocols included the following: axial T1-weighted spin-echo images (repetition time [TR], 580 milliseconds; echo time [TE],7.8 milliseconds; slice thickness, 5 mm; intersection space, 1 mm; and number of excitations [NEX], 2); and axial T2-weighted spin-echo images with fat suppression (TR, 6289 milliseconds; TE, 85 milliseconds; slice thickness, 5 mm; intersection space, 1 mm; and NEX, 2).

Single-shot diffusion-weighted spin-echo echo-planar (SE-DW-EPI) sequence was used to gather IVIM-DWI data, with 22-cm field of view, 5-mm slice thickness, 1-mm slice gap, 4225-millisecond TR, 106-millisecond TE, 128×130 matrix, and 4 NEX. A total of 12 axial slices covering the nasopharynx were obtained. Ten *b* values (0, 50, 80, 100, 150, 200, 400, 600, 800, and 1000 s/mm^2) were applied in the IVIM-DWI data acquisition. A local shim box covering the nasopharyngeal region was applied to minimize susceptibility artifacts.

2.3. IVIM-DWI parametric maps acquisition

All IVIM-DWI data were transferred to the Advantage Workstation (version AW 4.6; GE Medical Systems, Milwaukee, WI) for postprocessing using the MADC kit, a software package for multiple ADC measurement. Four IVIM-DWI parametric (ADC; pure diffusion coefficient, *D*; pseudo-diffusion coefficient, D^*; perfusion fraction, *f*) maps of each primary NPC lesion were generated on the basis of a pixel-by-pixel fitting according to the Levenberg–Marquardt algorithm.[31]

2.4. IVIM-DWI parametric values measurement

To determine the scope of each tumor, one radiologist (WL with 10 years of experience in head and neck MRI) who was blinded to the clinical and pathologic results and the treatment response manually traced the outer edge of the lesion on each axial ADC map with reference to the T2-weighted image, and the corresponding 2-dimensional (2D) region of interest (ROI) for each map was acquired. Both the most superior and the most inferior slices for each tumor were excluded to avoid volume averaging. Based on all the ROIs of this tumor, the MADC kit automatically generated a 3-dimensional (3D) volume of interest (VOI) for this tumor and output the volume datum and the mean ADC value of this VOI. The same VOI was also automatically copied and pasted by this software onto all the other IVIM-DWI maps, and the corresponding parametric values were obtained. Subsequently, these axial maps with ROI were saved as BMP format images for texture analysis.

2.5. Texture analysis

All the BMP format images were transferred into the MaZda program (http://www.eletel.p.lodz.pl/programy/mazda/index.php?action=mazda) for texture analysis. Because the ROIs in the IVIM-DWI maps cannot be utilized automatically by MaZda, one radiologist (WL) carefully manually traced the border of these original ROIs to generate new ROIs for texture analysis. Subsequently, a VOI for each tumor was generated automatically based on these new ROIs. For each VOI, gray-level normalization was performed by using $\mu \pm 3\sigma$ (μ, gray-level mean; σ, gray-level standard deviation), to minimize the influence of contrast and brightness variation. For each IVIM-DWI parametric map, 11 GLCM features were extracted automatically from the VOI by MaZda, including Angular Second Moment (AngScMom), Contrast, Correlat, Difference Entropy (DifEntrp), Difference Variance (Difvarnc), Entropy, Inverse Difference Moment (InvDfMom), Sum Average (SumAverg), Sum Entropy (SumEntrp), Sum of Squares (SumOfSqs), and Sum Variance (SumVarnc).

2.6. Sample size estimation

The sample size was calculated according to the formula $n = (U\alpha/\delta)/P\,(1-P)$. The allowable error ($\delta$) was set to 10%.The residual lesion rate (*P*) was supposed to 35%, according to our prior data.[11] The significance level (α) was defined as 0.05, and the critical value of $U\alpha$ as 1.96; therefore, $n = 86$. The eventual sample size was 90, allowing for loss of up to 5% of the patients.

2.7. Statistical analysis

All statistical analyses were done through SPSS version 22.0 (SPSS Inc, Chicago, IL) or MedCalc v15.0 software (MedCalc Software bvba, Ostend, Belgium). A 2-tailed test pattern was used in all statistical analyses with the level of statistical significance determined as $P < .05$. Categorical variables (gender, Tumor-Node-Metastasis [TNM] stage, and pathologic grade) were presented as frequency, and were compared using the Chi-squared test. Continuous variables (age, tumor volume, and the values of IVIM-DWI parameters and GLCM features) were expressed as mean ± standard deviation. The nonparametric Mann–Whitney *U* test was used in univariate analysis to explore the possible differences in continuous variables between the residue and nonresidue groups. Subsequently, multivariate logistic regression analysis (forward stepwise, LR; probability for stepwise entry, 0.05; removal, 0.1) was performed to identify the independent prognostic factors, using the indicators with statistical significance ($P < .05$) in univariate analysis as input variables. The discrimination power of the individual GLCM features and multivariate regression model for predicting the therapeutic response was determined with receiver operating characteristic (ROC) curve analysis.

3. Results

Of the initially enrolled 90 patients, 9 were eliminated because of serious image distortion (n = 3), dental artifacts (n = 3), withdrawal by patients (n = 1), or receiving other antitumor therapy after the end of chemoradiotherapy (n = 2) (Fig. 1). Thus, this study eventually included the remaining 81 patients whose clinical and pathologic characteristics are shown in Table 1. At the end of chemoradiotherapy, 11 patients were found with residual lesion and 70 were not.

There was no significant difference in age, gender, clinical stage, and pathologic grade between the residue and nonresidue groups (Table 1). Significantly larger baseline tumor volume was found for the residue group than for the nonresidue group ($P = .035$). In regard to the IVIM-DWI parametric values, the nonresidue group exhibited obviously lower ADC and *D* values (all $P < .01$) than the residue group, whereas D^* and *f* did not show significant difference between the 2 groups (Table 2). Among those 44 GLCM features extracted from the IVIM-DWI maps, 10 of them showed distinct difference between the 2 groups (Tables 3–6). The nonresidue group exhibited lower $\text{Correlat}_{\text{ADC}}$, Correlat_D, $\text{InvDfMom}_{\text{ADC}}$, InvDfMom_D, and InvDfMom_{D^*} values, together with higher Contrast_D, Contrast_f, $\text{SumAverg}_{\text{ADC}}$, SumAverg_D, and SumAverg_{D^*} values, than the

Table 1

Patient's clinical and pathologic characteristics.

Characteristic	Whole cohort (n = 81)	Residue group (n = 11)	Nonresidue group (n = 70)	*P*
Age, y	48.43 ± 12.03	48.91 ± 11.63	48.36 ± 12.17	.889
Tumor volume, mm^3	3396.68 ± 3997.54	5746.19 ± 5634.52	3027.47 ± 3592.84	.035
Gender				.530
Male	56	9	47	
Female	25	2	23	
Pathologic grade				.983
Undifferentiated	55	8	47	
Differentiated	26	3	23	
T stage				.092
T1	2	0	2	
T2	30	4	26	
T3	26	3	23	
T4	23	4	19	
N stage				.534
N0	2	0	2	
N1	6	1	5	
N2	56	6	50	
N3	17	4	13	
M stage				.633
M0	79	11	68	
M1	2	0	2	

residue group (all $P < .05$). Figure 2 shows 2 examples of MRIs for patients with NPC with different responses.

Based on ROC curve in univariate analysis, the area under the curve (AUC) values for individual GLCM features in the prediction of the treatment response ranged from 0.635 to 0.879, with sensitivities from 54.55% to 100.00% and specificities from 52.86% to 85.71% (Table 7). Among the 10 individual predictors, $InvDfMom_D$ had the highest specificity (100.00%), $InvDfMom_{ADC}$ owned the best specificity (85.71%), whereas $SumAverg_D$ exhibited the highest AUC value (0.879), followed by $InvDfMom_{ADC}$ (AUC = 0.865) and $SumAverg_{ADC}$ (AUC = 0.861). Multivariate logistic regression analysis demonstrated D ($P = .026$), $InvDfMom_{ADC}$ ($P = .033$), and $SumAverg_D$ ($P = .015$) as the independent predictors for identifying NPC without residue, with an AUC value of 0.977, a sensitivity of 90.91% and a specificity of 95.71%.

4. Discussion

This study focused on the performance of GLCM texture analysis based on IVIM-DWI on predicting the early response to chemoradiotherapy for patients with NPC. Our data showed that NPC lesions with residue after chemoradiotherapy differs from those without in the pretreatment GLCM features related to IVIM-DWI, which demonstrates the potential of GLCM analysis to predict the curative effect for NPC. Our observations also revealed that GLCM analysis might facilitate more IVIM-DWI parameters (ie, D^* and f) to obtain the capacity for predicting the treatment response of NPC. Moreover, the diffusion-related IVIM-DWI maps may be superior to the perfusion-related ones in terms of providing GLCM features for predicting the early response of NPC to chemoradiotherapy.

Table 2

Differences in the values of IVIM-DWI parameters between the residue and nonresidue groups.

Parameter	Residue (n = 11)	Nonresidue (n = 70)	*P*
ADC, $\times 10^{-3}$ mm^2/s	1.050 ± 0.220	0.899 ± 0.163	.018
D, $\times 10^{-3}$ mm^2/s	0.825 ± 0.172	0.659 ± 0.119	.002
D^*, $\times 10^{-3}$ mm^2/s	19.289 ± 13.268	17.814 ± 13.422	.461
f	0.279 ± 0.142	0.269 ± 0.079	.847

ADC = apparent diffusion coefficient, D^* = pseudo-diffusion coefficient, D = pure diffusion coefficient, f = perfusion fraction, IVIM-DWI = intravoxel incoherent motion diffusion-weighted imaging.

The present study demonstrated that Contrast, Correlat, InvDfMom, and SumAverg could serve as MRI biomarkers to differentiate between the residual and nonresidual NPC lesions before the start of chemoradiotherapy. Among the above GLCM features strongly correlated to treatment response, Contrast and InvDfMom are descriptors of tissue heterogeneity, while Correlation and SumAverg are not directly related to heterogeneity, according to the GLCM algorithm.[29,32] Lower InvDfMom or higher Contrast value indicates more heterogeneity.[25,27] In the present study, the nonresidue NPC group had higher $Contrast_D$ and $Contrast_f$ values, as well as lower $InvDfMom_{ADC}$, $InvDfMom_D$, and $InvDfMom_{D^*}$ values, than the residue group, indicating that NPC with more heterogeneity on the IVIM-DWI maps before treatment might be associated with better response to chemoradiotherapy. Similar to our observation, several studies also reported that malignancies with higher heterogeneity on clinical imaging maps might have better therapeutic response in a variety of tumors.[25,29,33] In a recent study,[29] malignant lymphomas demonstrating complete metabolic responders (CMRs) to chemotherapy reportedly showed higher pretreatment Contrast value on the standard uptake value map derived from ^{18}F-FDG PET-CT than those of non-CMR. A prior report[33] revealed that hepatocellular carcinomas with complete response (CR) after transcatheter arterial chemoembolization exhibited higher Moments (a GLCM feature that is virtually the opposite of homogeneity, namely higher Moments value represents lower homogeneity) value on the pretherapeutic iohexol-enhanced CT images than those with non-CR. Teruel et al[34] also found that breast cancer lesions achieving CR to

Table 3

Differences in the GLCM features values from ADC map between the residue and nonresidue groups.

Texture feature	Residue (n = 11)	Nonresidue (n = 70)	P
$AngScMom_{ADC}$	0.017 ± 0.014	0.013 ± 0.009	.473
$Contrast_{ADC}$	54.815 ± 14.536	64.185 ± 15.591	.071
$Correlat_{ADC}$	0.805 ± 0.031	0.759 ± 0.070	.034
$DifEntrp_{ADC}$	1.082 ± 0.090	1.115 ± 0.089	.270
$DifVarnc_{ADC}$	29.574 ± 5.567	32.912 ± 4.981	.082
$Entropy_{ADC}$	2.165 ± 0.151	2.145 ± 0.169	.473
$InvDfMom_{ADC}$	0.420 ± 0.167	0.195 ± 0.122	<.001
$SumAverg_{ADC}$	50.914 ± 9.185	60.810 ± 6.351	<.001
$SumEntrp_{ADC}$	1.681 ± 0.100	1.669 ± 0.097	.526
$SumOfSqs_{ADC}$	139.177 ± 21.489	136.796 ± 23.856	.783
$SumVarnc_{ADC}$	501.894 ± 74.209	482.999 ± 94.947	.491

ADC = apparent diffusion coefficient, GLCM = gray-level co-occurrence matrix.

Table 5

Differences in the GLCM features values from D^* map between the residue and nonresidue groups.

Texture feature	Residue (n = 11)	Nonresidue (n = 70)	P
$AngScMom_{D^*}$	0.011 ± 0.006	0.010 ± 0.005	.934
$Contrast_{D^*}$	55.534 ± 14.177	62.681 ± 13.966	.210
$Correlat_{D^*}$	0.804 ± 0.048	0.779 ± 0.069	.335
$DifEntrp_{D^*}$	1.102 ± 0.094	1.130 ± 0.069	.482
$DifVarnc_{D^*}$	29.222 ± 4.969	31.783 ± 5.297	.205
$Entropy_{D^*}$	2.240 ± 0.127	2.187 ± 0.148	.195
$InvDfMom_{D^*}$	0.362 ± 0.082	0.304 ± 0.067	.035
$SumAverg_{D^*}$	50.026 ± 5.031	56.112 ± 5.889	.002
$SumEntrp_{D^*}$	1.741 ± 0.057	1.196 ± 0.092	.104
$SumOfSqs_{D^*}$	143.036 ± 18.621	148.776 ± 34.958	.901
$SumVarnc_{D^*}$	516.609 ± 70.516	532.424 ± 138.960	.945

D^* = pseudo-diffusion coefficient, GLCM = gray-level co-occurrence matrix.

chemotherapy had higher baseline Contrast and Entropy (Entropy is a texture feature representing tissue heterogeneity) values on the 1-, 2-, and 3-minute postgadolinium T1-weighted MRIs than those with a response of stable disease according to the Response Evaluation Criteria in Solid Tumors (RECIST) v1.1. Nevertheless, contrary finding was reported in another study on breast cancer in which the responders (ie, with a chemotherapy-induced decrease in tumor diameter of >50%) demonstrated lower baseline Contrast value on the T1-weighted MRIs after administration of gadolinium agent, compared with the nonresponders.[27] These conflicting findings might result from the differences in the imaging protocols and treatment methods, especially from the great variations with regard to the classification of response across studies.[27,34]

The IVIM-DWI can simultaneously extract diffusion and perfusion information from viable tissues.[6,11,12] Among the 4 IVIM-DWI parameters, both D^* and f are related to microcirculation perfusion, while D is associated with pure diffusion.[6,11,12] ADC represents the total diffusion in viable tissues and is mainly related to diffusion rather than perfusion under the condition of b values >200 s/mm^2.[11,12,35] In regard to the four IVIM-DWI parameters, our data indicated that all of them could provide baseline GLCM features to predict the early outcome of chemoradiotherapy for NPC. Our data demonstrated that the pretreatment ADC and D values had the potential to predict the early-term treatment response for NPC, while D^* and f had not, which is in line with several prior studies.[11,12,15] In the present and previous studies,[11,12,15] the performance of D^* and f on differentiating curative effect was based on measure of mean IVIM-DWI parametric value instead of on texture analysis. Thus, it could be inferred that GLCM texture analysis may improve the performance of the perfusion-related IVIM-DWI parameters on the prediction of therapeutic effect for NPC, compared with the traditional average-based IVIM-DWI analysis.

In the univariate analysis in this study, the majority (7/10, 70.0%) of the GLCM features predictive of therapeutic response were generated from the diffusion-related IVIM-DWI parametric maps, whereas only 3 (3/10, 30.0%) from the perfusion-related maps. Moreover, the 10 predictors in this study belonged to 4 kinds of GLCM features, namely Contrast, Correlat, InvDfMom, and SumAverg. As for Correlat, all the 2 predictors were extracted from the ADC and D maps instead of from the D^* or f maps. In terms of Contrast, InvDfMom, and SumAverg, although both the diffusion- and perfusion-related IVIM-DWI maps could provide predictor for therapeutic effect, the AUC value of each individual predictor from the diffusion-related maps was higher than that from the perfusion-related maps, for example, $InvDfMom_D$ (AUC = 0.844) versus $InvDfMom_{D^*}$ (AUC = 0.699). Furthermore, multivariate analysis demonstrated that all the independent predictors (ie, D, $InvDfMom_{ADC}$, and $SumAverg_D$) were generated from the ADC or D map, rather than from the D^* and f maps. Similar to the findings of this study, previous reports based on an analysis of mean parametric value have revealed that the diffusion-related IVIM-DWI indices were

Table 4

Differences in the GLCM features values from *D* map between the residue and nonresidue groups.

Texture feature	Residue (n = 11)	Nonresidue (n = 70)	P
$AngScMom_D$	0.017 ± 0.015	0.013 ± 0.008	.424
$Contrast_D$	50.661 ± 10.544	61.786 ± 14.486	.021
$Correlat_D$	0.805 ± 0.039	0.753 ± 0.066	.012
$DifEntrp_D$	1.068 ± 0.095	1.112 ± 0.083	.129
$DifVarnc_D$	28.656 ± 4.142	31.679 ± 4.788	.137
$Entropy_D$	2.159 ± 0.148	2.131 ± 0.161	.308
$InvDfMom_D$	0.449 ± 0.082	0.321 ± 0.083	<.001
$SumAverg_D$	51.298 ± 5.252	59.450 ± 5.570	<.001
$SumEntrp_D$	1.682 ± 0.090	1.654 ± 0.095	.177
$SumOfSqs_D$	134.206 ± 18.105	128.075 ± 22.385	.363
$SumVarnc_D$	484.345 ± 64.451	450.513 ± 88.216	.168

D = pure diffusion coefficient, GLCM = gray-level co-occurrence matrix.

Table 6

Differences in the GLCM features values from *f* map between the residue and nonresidue groups.

Texture feature	Residue (n = 11)	Nonresidue (n = 70)	P
$AngScMom_f$	0.014 ± 0.007	0.013 ± 0.009	.378
$Contrast_f$	46.475 ± 10.035	55.957 ± 13.672	.032
$Correlat_f$	0.840 ± 0.046	0.829 ± 0.052	.544
$DifEntrp_f$	1.079 ± 0.071	1.102 ± 0.072	.349
$DifVarnc_f$	27.734 ± 3.393	29.712 ± 5.953	.378
$Entropy_f$	2.189 ± 0.126	2.142 ± 0.164	.363
$InvDfMom_f$	0.358 ± 0.074	0.328 ± 0.072	.225
$SumAverg_f$	39.933 ± 5.298	41.939 ± 6.978	.440
$SumEntrp_f$	1.714 ± 0.070	1.683 ± 0.095	.282
$SumVarnc_f$	164.536 ± 36.790	168.861 ± 29.911	.783
$SumOfSqs_f$	608.033 ± 147.382	619.485 ± 119.054	.710

f = perfusion fraction, GLCM = gray-level co-occurrence matrix.

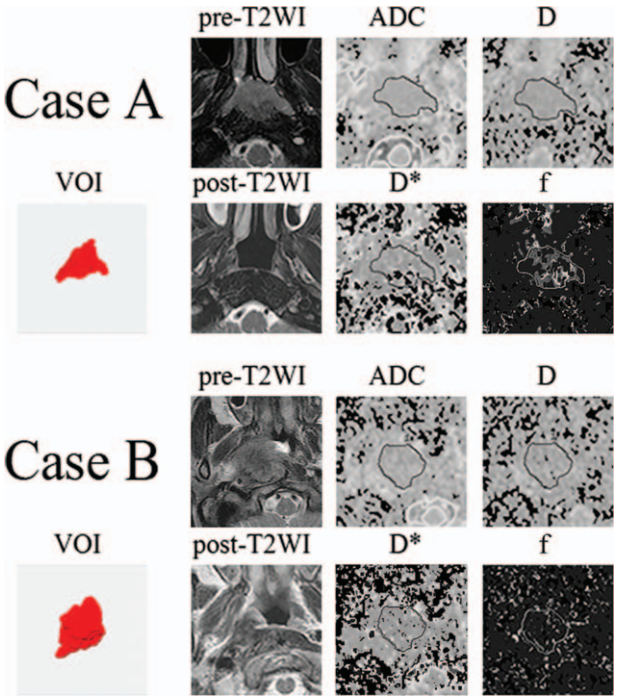

Figure 2. Examples of baseline intravoxel incoherent motion diffusion-weighted imaging (IVIM-DWI) maps, VOI for texture features extraction, and pre- and posttherapy T2WI images for nasopharyngeal carcinoma. The upper 2 rows show images from a patient (case A) in the nonresidue group, whereas the lower 2 rows exhibit images from a patient (case B) in the residue group. For case A, the primary lesion disappeared at the end of chemoradiotherapy, its baseline $Contrast_D$, $Contrast_f$, $Correlat_{ADC}$, $Correlat_D$, $DifVarnc_{ADC}$, $DifVarnc_D$, $InvDfMom_{ADC}$, $InvDfMom_D$, $InvDfMom_{D^*}$, $SumAverg_{ADC}$, $SumAverg_D$, and $SumAverg_{D^*}$ values were 63.738, 56.015, 0.711, 0.698, 34.892, 34.361, 0.245, 0.257, 0.328, 62.340, 63.267, and 60.157, respectively. For case B, the nasopharyngeal tumor demonstrated residue at the end of chemoradiotherapy, its baseline $Contrast_D$, $Contrast_f$, $Correlat_{ADC}$, $Correlat_D$, $DifVarnc_{ADC}$, $DifVarnc_D$, $InvDfMom_{ADC}$, $InvDfMom_D$, $InvDfMom_{D^*}$, $SumAverg_{ADC}$, $SumAverg_D$, and $SumAverg_{D^*}$ values were 52.135, 45.632, 0.773, 0.784, 26.876, 25.178, 0.401, 0.423, 0.387, 45.867, 49.376, and 48.763, respectively. ADC = apparent diffusion coefficient, D^* = pseudo-diffusion coefficient, D = true-diffusion coefficient, f = perfusion fraction, IVIM-DWI = intravoxel incoherent motion diffusion-weighted imaging, post-T2WI = posttreatment T2-weighted imaging, pre-T2WI = pretreatment T2-weighted imaging, VOI = volume of interest.

more powerful than the perfusion-related ones in the pretreatment prediction of response to chemoradiotherapy for NPC.[11,12] Taken together, these observations might signify that the pretreatment diffusion-related IVIM-DWI indices have an advantage over the perfusion-related ones in the early prediction of the curative effect in patients with NPC, whether based on texture analysis or average parametric value.

In this study, we explored the routine MRI findings (ie, tumor volume and TNM stage that indicates the degree of tumor progression), IVIM-DWI mean-parameter-value analysis and IVIM-DWI texture analysis for predicting NPC with lesion residue. The residue and nonresidue groups did not differ from each other in the TNM stage, suggesting that the clinical stage is of little benefit to predict the early response of NPC. In this study, NPC with larger baseline tumor volume was found more likely to appear residue at the end of chemoradiotherapy, which implied that tumor volume may serves as an indicator to predict the early chemoradiotherapy effect for NPC. Nevertheless, among all the 13 individual indicators in the prediction of tumor residue in the present study, tumor volume exhibited the lowest AUC value (0.635). Additionally, in the multivariate analysis in this study, it is the functional MRI indices (ie, D and texture features derived from IVIM-DWI maps), rather than tumor volume, that acted as the independent predictors to the treatment outcome of NPC. Moreover, this multivariate model had a significantly higher AUC value than tumor volume (AUC, 0.977 vs 0.635; $P = .002$). These observations strengthened the opinion that functional MRI approach may be more powerful than morphologic MRI methods in predicting chemoradiotherapy efficacy of malignancies including NPC.

Table 7

Performance of predictors on the differentiation between the residue and nonresidue groups in univariate analysis.

Predictor	Cut-off value	Sensitivity	Specificity	AUC (95% CI)
Tumor volume	3958.656 mm^3	54.55%	78.57%	0.635 (0.521–0.739)
ADC	0.902×10^{-3} mm^2/s	81.82%	55.71%	0.723 (0.613–0.817)
D	0.722×10^{-3} mm^2/s	72.73%	72.86%	0.791 (0.686–0.873)
$Contrast_D$	56.695	72.73%	62.86%	0.717 (0.606–0.811)
$Contrast_f$	51.523	72.73%	64.29%	0.703 (0.591–0.799)
$Correlat_{ADC}$	0.770	90.91%	52.86%	0.700 (0.588–0.797)
$Correlat_D$	0.768	90.91%	60.00%	0.738 (0.628–0.829)
$InvDfMom_{ADC}$	0.305	81.82%	85.71%	0.865 (0.567–0.913)
$InvDfMom_D$	0.339	100.00%	60.00%	0.844 (0.747–0.915)
$InvDfMom_{D^*}$	0.336	75.45%	70.00%	0.699 (0.587–0.796)
$SumAverg_{ADC}$	56.462	81.82%	82.86%	0.861 (0.766–0.928)
$SumAverg_D$	55.769	90.91%	74.29%	0.879 (0.788–0.941)
$SumAverg_{D^*}$	51.011	63.64%	85.71%	0.791 (0.686–0.873)

ADC = apparent diffusion coefficient, AUC = area under the curve, CI = confidence interval, D^* = pseudo-diffusion coefficient, D = pure diffusion coefficient, f = perfusion fraction.

There are several limitations in our study. First, we did not analysis the posttreatment GLCM features from the IVIM-DWI maps for NPC, which may result in insufficient discuss on the correlation between the therapeutic response and IVIM-DWI-based texture features for NPC. Second, we did not perform an analysis of a subgroup of patients stratified by TNM stages because of the relatively small sample size of certain stage subgroups, for example, the T1, N0, N1, and M1 subsets. In addition, the long-term outcome of NPC receiving chemoradiotherapy had not been evaluated in the present study. Therefore, further studies with larger patient population, long-term follow-up, stratification by clinical stage, and analysis of posttreatment IVIM-DWI-based texture features are warranted to comprehensively understand the relevance between the texture features and therapeutic effect for NPC.

In conclusion, the observations in this study indicated that GLCM features based on IVIM-DWI, especially on the diffusion-related map, may be a potential tool for predicting the early response of NPC before starting chemoradiotherapy.

Acknowledgment

The authors thank Mr Zhang Zhong-ping (GE Healthcare China, Beijing, China) for his assistance in MRI analysis.

Author contributions

Conceptualization: Xiaoping Yu.
Data curation: Yi Fu.
Investigation: Jing Hou, Ying Hu, Feiping Li, Lu Wen, Qiang Lu.
Methodology: Jing Hou, Feiping Li, Lu Wen, Qiang Lu.

Supervision: Ying Hu.
Validation: Siye Liu.
Writing – original draft: Yuhui Qin.
Writing – review & editing: Xiaoping Yu.

References

[1] Yu MC, Yuan JM. Epidemiology of nasopharyngeal carcinoma. Semin Cancer Biol 2002;12:421–9.
[2] Wei KR, Zheng RS, Zhang SW, et al. Nasopharyngeal carcinoma incidence and mortality in China, 2013. Chin J Cancer 2017;36:90.
[3] Zhang L, Chen QY, Liu H, et al. Emerging treatment options for nasopharyngeal carcinoma. Drug Des Devel Ther 2013;7:37–52.
[4] National Comprehensive Cancer Network. NCCN Clinical Practice Guidelines in Oncology: Head and Neck Cancers, V.2.2017. Available at https://www.nccn.org/professionals/physician_gls/pdf/head-and-neck.pdf. Accessed December 31, 2017.
[5] Lee AW, Sze WM, Au JS, et al. Treatment results for nasopharyngeal carcinoma in the modern era: the Hong Kong experience. Int J Radiat Oncol Biol Phys 2005;61:1107–16.
[6] Lai V, Li X, Lee VH, et al. Nasopharyngeal carcinoma: comparison of diffusion and perfusion characteristics between different tumour stages using intravoxel incoherent motion MR imaging. Eur Radiol 2014;24:176–83.
[7] Huang B, Wong CS, Whitcher B, et al. Dynamic contrast-enhanced magnetic resonance imaging for characterising nasopharyngeal carcinoma: comparison of semiquantitative and quantitative parameters and correlation with tumour stage. Eur Radiol 2013;23:1495–502.
[8] Chen Y, Liu X, Zheng D, et al. Diffusion-weighted magnetic resonance imaging for early response assessment of chemoradiotherapy in patients with nasopharyngeal carcinoma. Magn Reson Imaging 2014;32:630–7.
[9] Abdel Khalek Abdel Razek A, King A. MRI and CT of nasopharyngeal carcinoma. AJR Am J Roentgenol 2012;198:11–8.
[10] Zhang Y, Liu X, Zhang Y, et al. Prognostic value of the primary lesion apparent diffusion coefficient (ADC) in nasopharyngeal carcinoma: a retrospective study of 541 cases. Sci Rep 2015;5:12242.
[11] Hou J, Yu X, Hu Y, et al. Value of intravoxel incoherent motion and dynamic contrast-enhanced MRI for predicting the early and short-term responses to chemoradiotherapy in nasopharyngeal carcinoma. Medicine (Baltimore) 2016;95:e4320.
[12] Xiao-ping Y, Jing H, Fei-ping L, et al. Intravoxel incoherent motion magnetic resonance imaging for predicting early response to induction chemotherapy and chemoradiotherapy in patients with nasopharyngeal carcinoma. J Magn Reson Imaging 2016;43:1179–90.
[13] Zheng D, Chen Y, Chen Y, et al. Early assessment of induction chemotherapy response of nasopharyngeal carcinoma by pretreatment diffusion-weighted magnetic resonance imaging. J Comput Assist Tomogr 2013;37:673–80.
[14] Hong J, Yao Y, Zhang Y, et al. Value of magnetic resonance diffusion-weighted imaging for the prediction of radiosensitivity in nasopharyngeal carcinoma. Otolaryngol Head Neck Surg 2013;149:707–13.
[15] Xiao Y, Pan J, Chen Y, et al. Intravoxel incoherent motion-magnetic resonance imaging as an early predictor of treatment response to neoadjuvant chemotherapy in locoregionally advanced nasopharyngeal carcinoma. Medicine (Baltimore) 2015;94:e973.
[16] Zhang B, Tian J, Dong D, et al. Radiomics features of multiparametric mri as novel prognostic factors in advanced nasopharyngeal carcinoma. Clin Cancer Res 2017;23:4259–69.
[17] Chan SC, Chang KP, Fang YD, et al. Tumor heterogeneity measured on F-18 fluorodeoxyglucose positron emission tomography/computed tomography combined with plasma Epstein-Barr Virus load predicts prognosis in patients with primary nasopharyngeal carcinoma. Laryngoscope 2017;127:E22–8.
[18] Wu J, Gong G, Cui Y, et al. Intratumor partitioning and texture analysis of dynamic contrast-enhanced (DCE)-MRI identifies relevant tumor subregions to predict pathological response of breast cancer to neoadjuvant chemotherapy. J Magn Reson Imaging 2016;44:1107–15.
[19] Henderson S, Purdie C, Michie C, et al. Interim heterogeneity changes measured using entropy texture features on T2-weighted MRI at 3.0 T are associated with pathological response to neoadjuvant chemotherapy in primary breast cancer. Eur Radiol 2017;27:4602–11.
[20] Liu J, Mao Y, Li Z, et al. Use of texture analysis based on contrast-enhanced MRI to predict treatment response to chemoradiotherapy in nasopharyngeal carcinoma. J Magn Reson Imaging 2016;44:445–55.
[21] Jansen JF, Lu Y, Gupta G, et al. Texture analysis on parametric maps derived from dynamic contrast-enhanced magnetic resonance imaging in head and neck cancer. World J Radiol 2016;8:90–7.
[22] De Cecco CN, Ciolina M, Caruso D, et al. Performance of diffusion-weighted imaging, perfusion imaging, and texture analysis in predicting tumoral response to neoadjuvant chemoradiotherapy in rectal cancer patients studied with 3T MR: initial experience. Abdom Radiol (NY) 2016;41:1728–35.
[23] Liu L, Liu Y, Xu L, et al. Application of texture analysis based on apparent diffusion coefficient maps in discriminating different stages of rectal cancer. J Magn Reson Imaging 2017;45:1798–808.
[24] Parikh J, Selmi M, Charles-Edwards G, et al. Changes in primary breast cancer heterogeneity may augment midtreatment MR imaging assessment of response to neoadjuvant chemotherapy. Radiology 2014;272:100–12.
[25] Haralick RM, Shanmugam K, Dinstein IH. Textural features for image classification. IEEE Trans Systems Man Cybernetics 1973;3:610–21.
[26] Thibault G, Tudorica A, Afzal A, et al. DCE-MRI texture features for early prediction of breast cancer therapy response. Tomography 2017;3:23–32.
[27] Ahmed A, Gibbs P, Pickles M, et al. Texture analysis in assessment and prediction of chemotherapy response in breast cancer. J Magn Reson Imaging 2013;38:89–101.
[28] Liu M, Lv H, Liu LH, et al. Locally advanced rectal cancer: predicting non-responders to neoadjuvant chemoradiotherapy using apparent diffusion coefficient textures. Int J Colorectal Dis 2017;32:1009–12.
[29] Ben Bouallègue F, Tabaa YA, Kafrouni M, et al. Association between textural and morphological tumor indices on baseline PET-CT and early metabolic response on interim PET-CT in bulky malignant lymphomas. Med Phys 2017;44:4608–19.
[30] Edge SB, Compton CC. The American Joint Committee on Cancer: the 7th edition of the AJCC cancer staging manual and the future of TNM. Ann Surg Oncol 2010;17:1471–4.
[31] Marquardt D. An algorithm for least-squares estimation of nonlinear parameters. SIAM J Appl Math 1963;11:431–41.
[32] Kolarevic D, Tomasevic Z, Dzodic R, et al. Early prognosis of metastasis risk in inflammatory breast cancer by texture analysis of tumour microscopic images. Biomed Microdevices 2015;17:92.
[33] Park HJ, Kim JH, Choi SY, et al. Prediction of therapeutic response of hepatocellular carcinoma to transcatheter arterial chemoembolization based on pretherapeutic dynamic CT and textural Findings. AJR Am J Roentgenol 2017;209:W211–20.
[34] Teruel JR, Heldahl MG, Goa PE, et al. Dynamic contrast-enhanced MRI texture analysis for pretreatment prediction of clinical and pathological response to neoadjuvant chemotherapy in patients with locally advanced breast cancer. NMR Biomed 2014;27:887–96.
[35] Dikaios N, Punwani S, Hamy V, et al. Noise estimation from averaged diffusion weighted images: can unbiased quantitative decay parameters assist cancer evaluation? Magn Reson Med 2014;71:2105–17.